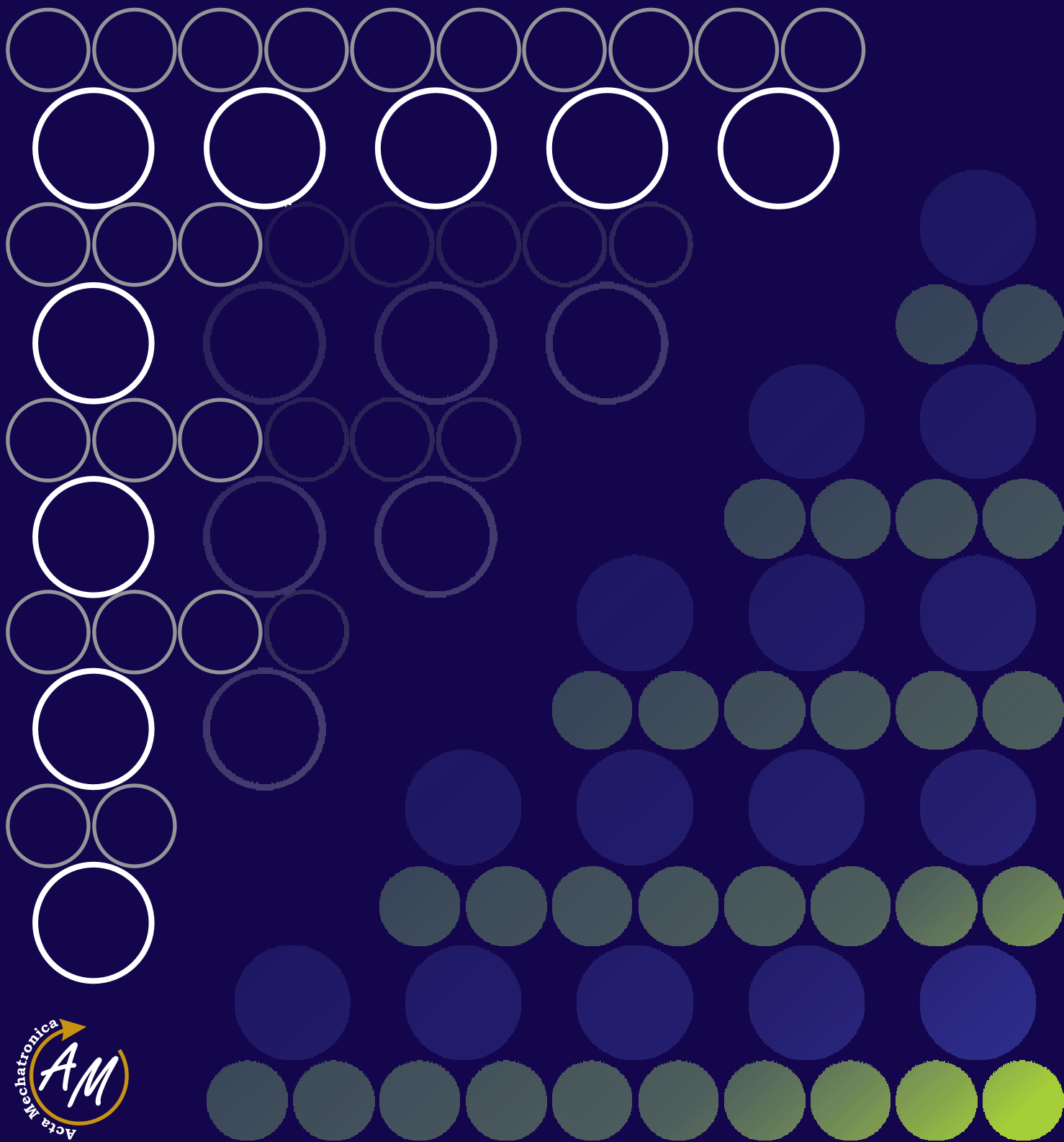


# ACTA MECHATRONICA

2021 Volume 6

Issue 4



International Scientific Journal about Mechatronics  
electronic journal  
ISSN 2453-7306

---

**CONTENTS**  
**(DECEMBER 2021)**

---

**(pages 51-56)**

**DETERMINING THE STRAIN SENSITIVITY OF RESISTANCE STRAIN  
GAUGES**

Ingrid Delyová, Darina Hroncová, Ján Kostka, Vojtech Neumann, Jana Bokorová

**(pages 57-61)**

**LINEAR SOLENOID ELECTROMAGNETIC ACTUATOR WITH  
DIFFERENTIAL SERIES WINDINGS**

Tatiana Kelemenová, Ivana Koláriková, Ondrej Benedik

**(pages 63-68)**

**SOFTWARE APPLICATION FOR A SYSTEM WITH A PROGRAMMABLE  
LOGIC CONTROLLER**

Jaroslav Romančík, Michal Kelemen

**DETERMINING THE STRAIN SENSITIVITY OF RESISTANCE STRAIN GAUGES**

Ingrid Delyová; Darina Hroncová; Ján Kostka; Vojtech Neumann; Jana Bokorová

doi:10.22306/am.v6i4.79

Received: 23 Oct. 2021

Revised: 19 Nov. 2021

Accepted: 10 Dec. 2021

**DETERMINING THE STRAIN SENSITIVITY OF RESISTANCE STRAIN GAUGES****Ingrid Delyová**

Department of Applied Mechanics and Mechanical Engineering, Faculty of Mechanical Engineering, Technical University of Košice, Park Komenského 8, 042 00 Košice, Slovakia, EU, ingrid.delyova@tuke.sk (corresponding author)

**Darina Hroncová**

Department of Mechatronics, Faculty of Mechanical Engineering, Technical University of Košice, Park Komenského 8, 042 00 Košice, Slovakia, EU, darina.hroncova@tuke.sk

**Ján Kostka**

Department of Applied Mechanics and Mechanical Engineering, Faculty of Mechanical Engineering, Technical University of Košice, Park Komenského 8, 042 00 Košice, Slovakia, EU, jan.kostka@tuke.sk

**Vojtech Neumann**

Department of Applied Mechanics and Mechanical Engineering, Technical University of Košice, Park Komenského 8, 042 00 Košice, Slovakia, EU, vojtech.neumann@student.tuke.sk

**Jana Bokorová**

Department of Mechatronics, Faculty of Mechanical Engineering, Technical University of Košice, Park Komenského 8, 042 00 Košice, Slovakia, EU, jana.bokorova@gmail.com

**Keywords:** strain gauge, k-factor, relative strain

**Abstract:** When measuring biaxial tension, it is necessary to measure the relative elongation in several directions, for which resistance strain gauges are used. Measurement with resistance strain gauges is based on the change in resistance of the electrical conductor when a deformation occurs. This paper discusses the design of a device for determining the strain sensitivity of resistive strain gauges, which we call the k-factor.

## 1 Introduction

Measurement with resistance strain gauges is based on the change in resistance of the electrical conductor under deformation. The change in conductivity of metals during deformation was discovered as early as 1856 by Thomson Lord Kelvin. In about 1937, A. Ruge in Massachusetts glued a wire to a paper backing and attached the ends of the wire to feeder wires of larger cross-section. This provided the basis for the manufacture of resistance strain gauges. The rapid development of the aerospace and automotive industries has increased the demands on experimental stress analysis. Resistive strain gauging was one of the avenues. This was driven by the development of new strain gauge apparatus and strain gauges for different purposes. The high measurement accuracy made them attractive in the field of sensor construction in measurement technology.

Measurement with resistance strain gauges is based on the change in resistance of the electrical conductor under deformation. The magnitude of the deformation of a structural element is determined from the change in resistance of the applied strain gauge on the surface under test, which is usually measured when connected to a Wheatstone bridge. Three basic types of strain gauges are used today. These are strain gauges with a wire which is adhered full length to a support, strain gauges in which the

winding is formed by etching a pattern from a thin foil, and finally strain gauges in which the wire is fixed by its ends to the support but is free throughout its length [1,2].

For biaxial strain measurements where it is necessary to measure the relative elongation in multiple directions, strain gauges are used that have three or four windings suitably oriented and bonded to a single pad. The windings may be glued not only side by side but also on top of each other. The material of the wire windings is usually chosen from copper-nickel alloy, or nickel-chromium, iron-nickel, or others as appropriate. Each kind has different properties in something. Some have greater sensitivity, others have a greater linear range, others have a higher allowable elongation, they also differ in their physical properties when the temperature changes, etc. [1-4].

### 1.1 Physical principles of resistance strain gauges

The strain gauge strain measurement is based on the assumption that the strain of the object under test is transmitted losslessly to the strain gauge. The prerequisite is a firm connection between the strain gauge and the object to be measured. In most cases, it can only be measured on free and unloaded surfaces of the measured objects. The required firm connection between the object to be measured and the strain gauge is best realized with a

**DETERMINING THE STRAIN SENSITIVITY OF RESISTANCE STRAIN GAUGES**

Ingrid Delyová; Darina Hroncová; Ján Kostka; Vojtech Neumann; Jana Bokorová

special adhesive. In the case of plastic objects or concrete structures, the strain gauge is cast into the model or concrete. In the latter case, special strain sensors in the form of a capsule are required. Other means and methods of fixing are mainly limited to special areas of application, such as ceramic means. For high temperature measurements, spot welding is used. In these cases, special strain gauges are required [3-5].

### 1.2 Measurement chain

The deformation transmitted from the measured object to the strain gauge causes a measurable change in electrical resistance in an electrical resistance strain gauge. The deformations to be measured by the strain gauge are usually very small, and as a result the changes in resistance are also very small and cannot be adequately measured by the direct use of an ohm meter. It is therefore necessary to use a so-called measuring chain, which allows the small resistance changes of the strain gauge to be determined accurately.

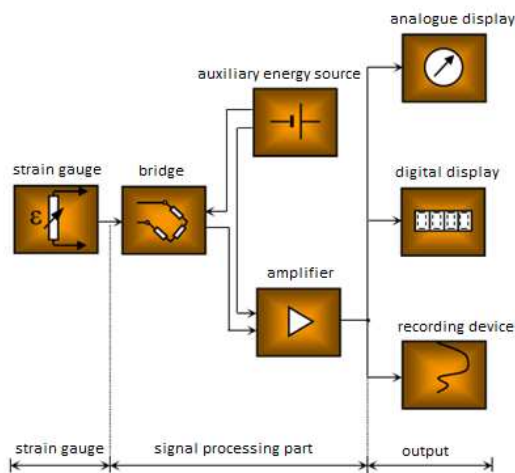


Figure 1 Measurement chain diagram for strain gauge measurement

The above description of the measurement chain shows only schematically the necessary parts. In practice, the measurement chain often contains various accessories such as a device for switching the measuring point, filters, memories for storing maximum values, recorders, etc. In addition, electronic data processing systems may be connected instead of indicating instruments, with various possible uses [2-5].

## 2 Strain sensitivity of resistance strain gauges

### 2.1 Longitudinal sensitivity

The operation of resistance strain gauges is based on the Wheatstone and Thomson effect of the interdependence of the relative strain and resistance in an electrical conductor. Each electrical conductor changes its resistance as a result of mechanical loading. The ohmic resistance  $R$

(1) of a resistive conductor depends directly on the conductor length  $l$ , the specific resistance  $\rho$  and indirectly on the cross-sectional area  $A$  ( $R = f(\rho, l, A)$ ) [1].

Thus

$$R = \rho \frac{l}{A} \quad (1)$$

The differential of the above function expresses the change in resistance (2)

$$\begin{aligned} dR &= \frac{\partial R}{\partial \rho} d\rho + \frac{\partial R}{\partial l} dl + \frac{\partial R}{\partial A} dA \\ &= \frac{l}{A} d\rho + \frac{\rho}{A} dl - \frac{\rho l}{A^2} dA \end{aligned} \quad (2)$$

The proportional change in conductor resistance is proportional to the proportional change in conductor length, then (3)

$$\frac{\frac{dR}{R}}{\frac{dl}{l}} = \frac{\frac{d\rho}{\rho} + \frac{dl}{l} - \frac{dA}{A}}{\frac{dl}{l}}, \quad (3)$$

where  $\frac{dl}{l} = \varepsilon$ , then strain sensitivity of resistance strain gauges  $k$ - factor is (4)

$$k = \frac{\frac{d\rho}{\rho} + \varepsilon - \frac{dA}{A}}{\varepsilon} \quad (4)$$

A fully satisfactory explanation for the change in resistivity has not yet been found. De Forest gives a linear dependence between the proportional change in resistance and the proportional change in length by the expression (5)

$$\frac{d\rho}{\rho} = \vartheta \frac{dl}{l} = \vartheta \varepsilon \quad (5)$$

Determine the relative change in cross-sectional area of the conductor, Figure 2

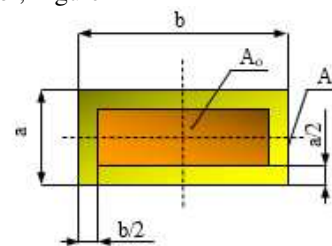


Figure 2 Change in conductor area before and after deformation

The change of area  $A_0$  will be (6)

$$\begin{aligned} A_0 &= (a - \Delta a)(b - \Delta b) \\ &= a \left(1 - \frac{\Delta a}{a}\right) b \left(1 - \frac{\Delta b}{b}\right) \end{aligned} \quad (6)$$

We know that  $\frac{\Delta a}{a}$  and  $\frac{\Delta b}{b}$  is the relative cross-sectional constriction of the conductor, for which we can write (7)

**DETERMINING THE STRAIN SENSITIVITY OF RESISTANCE STRAIN GAUGES**

Ingrid Delyová; Darina Hroncová; Ján Kostka; Vojtech Neumann; Jana Bokorová

$$\frac{\Delta a}{a} = \frac{\Delta b}{b} = \mu\varepsilon. \quad (7)$$

According to the infinitesimal calculus, we can neglect the very small terms in the above expression ( $\mu^2\varepsilon^2 \approx 0$ ), the relative change in area will be

$$\frac{dA}{A} = \frac{A_0 - A}{A} = \frac{A(1 - 2\mu\varepsilon) - A}{A} = -2\mu\varepsilon. \quad (8)$$

Equation (8) is substituted into (4) to obtain

$$k = \vartheta + 1 + 2\mu. \quad (9)$$

In equation (9) for the plastic region,  $\vartheta \approx 0$  holds

Bridgman, in his investigation of high pressures in liquids as early as 1917, pointed out the linear dependence of the change in resistance on the all-round pressure, i.e., on the change in the volume of the conductor (10).

$$\frac{d\rho}{\rho} = c \frac{dV}{V}. \quad (10)$$

The volume of the conductor  $V = Al$  is a function of the variables  $V = f(A, l)$ , for which we can construct a differential equation of the form (11)

$$dV = \frac{\partial V}{\partial A} dA + \frac{\partial V}{\partial l} dl = l dA + A dl. \quad (11)$$

Then we get the  $k$ -factor in the form (12)

$$k = \frac{\frac{d\rho}{\rho} + \varepsilon - \frac{dA}{A}}{\varepsilon} = c(1 - 2\mu) + 1 + 2\mu. \quad (12)$$

Since Bridgmann's constant  $c$  is constant for a certain material type and processing, the deformation coefficient in this case is just a function of the Poisson number. The expression  $c(1 - 2\mu)$  represents the piezoresistive phenomenon characteristic of semiconductors. The expression  $(1 + 2\mu)$  represents the deformation phenomenon characteristic of electrical conductors.

## 2.2 Transverse sensitivity

Strain gauges should respond by changing resistance to deformation only in their active direction. The term 'active direction' should be understood for resistance strain gauges to always be in the direction of measurement or the resistance filament of the strain gauge.

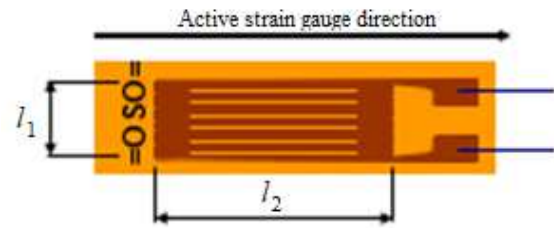


Figure 3 Active strain gauge direction

Consider a winding that is simplified so that the loop is formed orthogonally. The length of the strain gauge is  $l_1$ , so the total length of the winding parallel to the longitudinal axis of the strain gauge is  $nl_1$ , if  $n$  is the number of wires [1].

The length of the strain gauge is determined by the dimension  $nl_1 + l_2 = l_{celk}$ , where  $l_1$  is the length of the active part of the strain gauge in the longitudinal direction and  $l_2$  is the length of the active part of the strain gauge in the transverse direction. Determine the proportional change in resistance [5,6]

$$\frac{\Delta R}{R} = k \frac{\Delta l_{celk}}{l_{celk}} = \frac{k}{l_{celk}} (\Delta l_1 + \Delta l_2), \quad (13)$$

where  $\Delta l_1$  is the total elongation of the strain gauge filament, i.e.  $\Delta l_1 = n_1 l_1 \varepsilon_1$  and  $\Delta l_2$  is the total shortening of the filament in the transverse direction, i.e.  $\Delta l_2 = l_2 \varepsilon_2$ . Let us denote by  $\varepsilon_1 = \varepsilon$ . Then, based on the dependence of the longitudinal elongation of the filament and the transverse shortening of the filament (14)

$$\varepsilon_2 = -\mu\varepsilon_1 = -\mu\varepsilon. \quad (14)$$

The proportional change in resistance can then be expressed as (15)

$$\begin{aligned} \frac{\Delta R}{R} &= \frac{k}{nl_1 + l_2} (n_1 l_1 \varepsilon_1 + l_2 \varepsilon_2) \\ &= \frac{k}{nl_1 + l_2} (n_1 l_1 \varepsilon - l_2 \mu\varepsilon) \end{aligned} \quad (15)$$

where

$$\begin{aligned} K_1 &= \frac{kn_1 l_1}{nl_1 + l_2}, \\ K_2 &= \frac{kl_2}{nl_1 + l_2}. \end{aligned} \quad (16)$$

then

$$\frac{\Delta R}{R} = K_1 \varepsilon - K_2 \mu\varepsilon = K\varepsilon, \quad (17)$$

$K = K_1(1 - \mu\chi)$  and  $\chi = \frac{K_2}{K_1}$  is the transverse sensitivity defined as the ratio of the strain sensitivity  $K_2$  perpendicular to the measurement direction and the strain sensitivity  $K_1$  in the measurement direction.

**DETERMINING THE STRAIN SENSITIVITY OF RESISTANCE STRAIN GAUGES**

Ingrid Delyová; Darina Hroncová; Ján Kostka; Vojtech Neumann; Jana Bokorová

**3 Determination of deflection of a beam with a constant internal bending moment**

Determination of the strain coefficient of a resistance strain gauge is most conveniently made by means of a beam subjected to pure bending. The condition for pure bending is that a constant bending moment  $M_o$  is applied in the internal cross-section of the beam.

Experimental determination of the  $k$ -factor requires determination of the deflection of such a beam.

The progression of the bending moment functions is shown in Figure 4

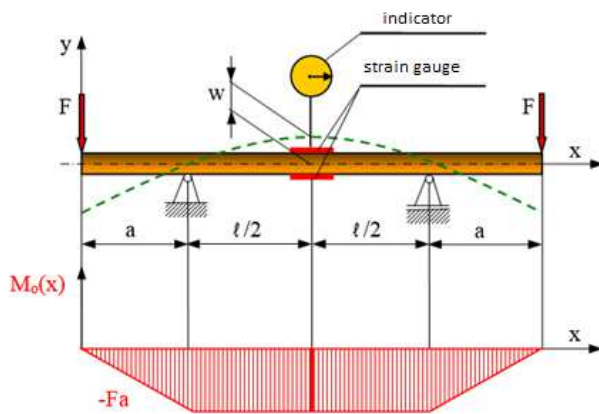


Figure 4 The course of bending moment functions

The deflection of a given beam is expressed by the relation (18)

$$w = -\frac{Fal^2}{8EJ_z}, \quad J_z = \frac{bh^3}{12}. \quad (18)$$

The deflection  $w$  itself can be determined by measurement on the beam, for example by using a needle indicator.

The force is (19)

$$F = -\frac{8EJ_z}{al^2}w = \frac{2Eb h^3}{3al^2}w, \quad (19)$$

where  $w$  is the value read from the needle indicator.

The next procedure in determining the  $k$ -factor requires knowing the relative fiber elongation at the point of strain gauge application. The relative fiber elongation can be determined from Hooke's law. The normal stress from bending in the region under study is (20)

$$\sigma = \frac{M_o}{W_{oz}} = -\frac{6Fa}{bh^2}, \quad (20)$$

where  $W_{oz} = bh^2/6$  is the cross-sectional modulus of the cross-section of the beam.

The relative deformation after adjustment will be (21)

$$\varepsilon = \frac{-Fa}{W_{oz}E} = \frac{4h}{l^2}w. \quad (21)$$

The  $k$ -factor is usually determined on strain gauges applied to a beam loaded in pure bending. Therefore, it is necessary to wire the strain gauge to sense only small strains due to bending to the exclusion of other types of stresses.

One strain gauge, is glued to the tension side of the beam and the other to the compression side of the beam (Figure 5).

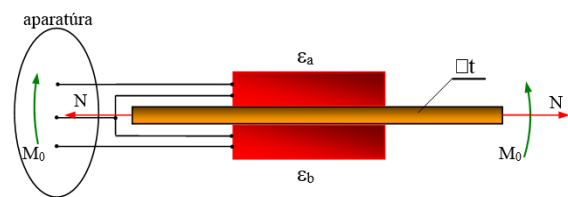


Figure 5 Strain gauge wiring for measuring bending stress excluding tension and temperature change

The strain gauges are connected to a Wheatson bridge, the schematic of which is shown in Figure 6.

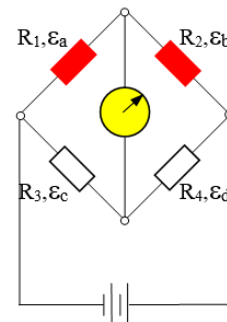


Figure 6 Wheatstone bridge diagram

The bridge consists of four resistive branches, a power supply and a sensitive galvanometer. In two of them we place the strain gauges. In the schematic they are labeled  $\varepsilon_a$ ,  $\varepsilon_b$  and are represented by resistors  $R_1$   $R_2$ . The stress increment on the galvanometer can be determined according to the relation (22)

$$dU_g == C(\varepsilon_a - \varepsilon_b - \varepsilon_c + \varepsilon_d), \quad (22)$$

where  $\varepsilon_i$ ,  $i = (a, b, c, d)$  are the resistances of the individual branches of the Wheatson bridge.

In the upper branches of the bridge, the resistance changes are due to changes in the length of the outermost fibres on the beam. They can be calculated as follows (23):

$$\begin{aligned} \varepsilon_a &= \varepsilon_t - \varepsilon_o + \varepsilon_T, \\ \varepsilon_b &= \varepsilon_t + \varepsilon_o + \varepsilon_T, \end{aligned} \quad (23)$$

**DETERMINING THE STRAIN SENSITIVITY OF RESISTANCE STRAIN GAUGES**

Ingrid Delyová; Darina Hroncová; Ján Kostka; Vojtech Neumann; Jana Bokorová

where  $\varepsilon_t$  is induced by tension,  $\varepsilon_o$  bending and  $\varepsilon_T$  by temperature change. The changes in resistance in the lower branches are equal to (24)

$$\varepsilon_c = 0, \quad \varepsilon_d = 0. \quad (24)$$

$\varepsilon_c$ ,  $\varepsilon_d$  are represented by resistors  $R_3$ ,  $R_4$  and are part of the apparatus. The above circuit is said to be a so-called half-bridge circuit.

By modifying equation (22) we get

$$dU_g = C(-2\varepsilon_o). \quad (25)$$

In the apparatus we use to measure the strain gauge deformation, we set an arbitrary value of the k-factor that is close to 2 and denote it by  $k_{ap}$ . We then read off the measured value of the relative strain  $\varepsilon_{ap}$  from the apparatus. We know that the relative change in resistance

$$\frac{\Delta R}{R} = k_{ap} \cdot \varepsilon_{ap} = k\varepsilon. \quad (26)$$

If the expression (21) is substituted into equation (26) for the proportional deformation, then, after adjustment, we get (27)

$$k = k_{ap} \frac{\varepsilon_{ap} l^2}{4hw}. \quad (27)$$

Rozmery obdĺžnikového priečného prierezu nosníka sme zvolili  $b = 20 \text{ mm}$  a  $h = 10 \text{ mm}$ .

The dimensions of the rectangular cross-section of the beam were chosen as  $b = 20 \text{ mm}$  and  $h = 10 \text{ mm}$ .



Figure 7 P-3500 and SB-10 Load Cell and Measuring Assembly

For the experiment, we used the SB-10 (SWITCH A BALANCE UNIT) junction box and the P-3500 (STRAIN INDICATOR) apparatus from Measurements group, Instruments division, Raleigh, NC (Figure 7). The system is designed for static measurements, with the option of connecting strain gauges to a quarter, half, or full bridge [7-11].

A description of the loading device is given in Figure 8. In this device, the load on the beam is induced by a load bolt.



Figure 8 Beam clamped to the loading device

Using the P-3500 apparatus, we read the values of the relative deformation  $\varepsilon_{ap}$  as a function of the deflection  $w_i$ . The measured values are shown in Table 1. The deflection  $w_i$  is read using a needle indicator.

Table 1 The measured values

Order of measurement	1	2	3	4	5	6	7	8	9	10
Measured quantity										
$w_i$ [mm]	5	10	15	20	25	30	35	40	45	50
$\varepsilon_{ap} \cdot 10^{-6}$	5.3	10.6	16.2	21.5	26.7	31.7	37.8	42.3	48.9	53.5

From the measured values shown in Table 1, we based the calculation of the actual relative deformation  $\varepsilon_{cal}$  and the corresponding value of the k-factor  $k_{cal}$ . The value of  $\varepsilon_{cal}$  (28) was calculated according to equation (21)

$$\varepsilon_{cal_i} = \frac{4h}{l^2} w_i. \quad (28)$$

The k-factor values for each measurement will be (29) (see Table 2)

$$k_{cal_i} = \frac{k_{ap} \cdot \varepsilon_{ap_i}}{\varepsilon_{cal_i}}. \quad (29)$$

Table 2 The calculated values

Order of measurement	1	2	3	4	5	6	7	8	9	10
Calculated quantity										
$\varepsilon_{cal_i}$	7.9	15.8	23.7	31.6	39.5	47.4	55.3	63.2	71.1	79
$k_{cal_i}$	1.87	1.88	1.85	1.86	1.87	1.89	1.85	1.89	1.84	1.87

The calculated magnitude of the k-factor was computed using a weighted average and is  $\bar{k}_{cal} = 1.88$ .

## 4 Conclusion

The proposed methodological solution procedure for determining the k-factor of strain gauges is correct. The strain device is fully compliant for the determination of the factor. Of course, there are other ways of determining the k-factor, but the above procedure is fast and efficient.

**DETERMINING THE STRAIN SENSITIVITY OF RESISTANCE STRAIN GAUGES**

Ingrid Delyová; Darina Hroncová; Ján Kostka; Vojtech Neumann; Jana Bokorová

Mastering this methodology provides a suitable tool for solving problems of teaching and practice.

**Acknowledgements**

This work was supported by the Ministry of Education of Slovakia Foundation under Grant project, VEGA No. 1/0290/18, VEGA No. 1/0389/18 and KEGA No.027TUKE-4/2020, KEGA 030 TUKE-4/2020.

**References**

- [1] RUZHA, Z.: *Electrical resistance strain gauges*, Praha, 1958. (Original in Slovak)
- [2] TREBUŇA, F., ŠIMČÁK, F., JURICA, V.: *Flexibility and strength I.*, Košice, Viena, 2000. (Original in Slovak)
- [3] TREBUŇA, F., ŠIMČÁK, F.: *Manual of Experimental Mechanics*, TypoPress, Košice, 2007. (Original in Slovak)
- [4] FRANKOVSKÝ, P., DELYOVÁ, I., SIVÁK, P., KURYLO, P., PIVARČIOVÁ, E., NEUMANN, V.: Experimental assessment of time-limited operation and rectification of a bridge crane, *Materials*, Vol. 13, No. 12, pp. 1-12, 2020.
- [5] BOCKO, J., DELYOVÁ, I., SIVÁK, P., TOMKO, M.: Selection of a significant numerical model of plasticity for the purpose of numerical analysis of plastic reinforcement, *American Journal of Mechanical Engineering*, Vol. 5, No. 6, pp. 334-340, 2017.
- [6] FANG, H., CHAN, T.M., YOUNG, B.: Material properties and residual stresses of octagonal high strength steel hollow sections, *Journal of Constructional Steel Research*, Vol. 148, pp. 479-490, 2018.
- [7] SU, Z., WU, H., CHEN, H., GUO, H., CHENG, X., SONG, Y., Zhang, H.: Digitalized self-powered strain gauge for static and dynamic measurement, *Nano Energy*, Vol. 42, pp. 129-137, 2017.
- [8] ZHANG, Z.T., Hu, S.J.: Stress and residual stress distributions in plane strain bending, *International Journal of Mechanical Sciences*, Vol. 40, No. 6, pp. 533-543, 1998.
- [9] SÁGA, M., KOPAS, P., UHRÍČIK, M.: Modeling and experimental analysis of the aluminium alloy fatigue damage in the case of bending-torsion loading, *Procedia Engineering*, Vol. 48, pp. 599-606, 2012.
- [10] TERTEL, E., KURYLO, P.: The stability of the sandwich conical shell panel-the stress state analysis, *Technical Gazette*, Vol. 24, No. 1, pp. 55-60, 2017.
- [11] KOSTKA, J., FRAKOVSKÝ, P., ČARÁK, P., NEUMANN, V.: Evaluation of residual stresses using optical methods, *Acta Mechatronica*, Vol. 4, No. 4, pp. 29-34, 2019.

**Review process**

Single-blind peer review process.

## LINEAR SOLENOID ELECTROMAGNETIC ACTUATOR WITH DIFFERENTIAL SERIES WINDINGS

**Tatiana Kelemenová**

Technical University of Kosice, Faculty of Mechanical Engineering, Letna 9, Kosice, Slovak Republic, EU,  
tatiana.kelemenova@tuke.sk (corresponding author)

**Ivana Koláriková**

Technical University of Kosice, Faculty of Mechanical Engineering, Letna 9, Kosice, Slovak Republic, EU,  
ivana.kolarikova@tuke.sk

**Ondrej Benedik**

Kybernetes, s.r.o., Omská 14, Kosice, Slovak Republic, EU,  
ondrej.benedik@kybernetes.sk

**Keywords:** actuator, solenoid, magnet, coil, force

**Abstract:** A linear solenoid electromagnetic actuator is a device for creating a linear reciprocating motion with a force effect. It contains a moving part consisting of a permanent magnet in the housing, threaded spacers, threaded rods, nuts for adjusting the stroke of the actuator and the hanging eyes of the actuator. The device further comprises a non-moving part formed by the coil body, the left actuator coil winding, the right actuator coil winding and the actuator cover, the sense of winding the left actuator coil winding opposite.

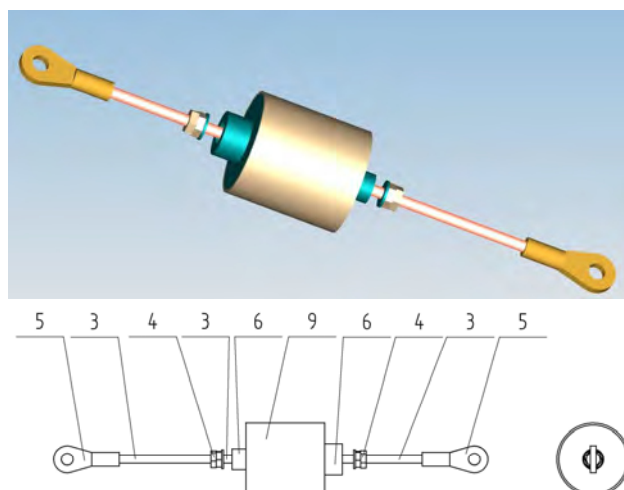
### 1 Introduction

Solenoid linear electromagnetic actuators are often used in mechatronic systems, which are mostly formed by a single coil and a ferromagnetic core which is inserted into the coil by an electromagnetic field. The return movement is provided by a spring. The disadvantage of such solutions is that the resulting force is smaller by the value of the force required to compress the spring. At the same time, when moving backwards, the force is limited by the value of the stiffness of the spring and its deformation [1-6].

### 2 Principle of operation

The linear solenoid electromagnetic actuator with differential series-connected windings and a permanent magnet is intended for the transformation of electrical energy into mechanical work in the form of a linear displacement with a force effect (Figure 1). The fundamental of this actuator lies in the fact that the electric current passing through the actuator coils and the magnetic field of the permanent magnet, thus causing mutual movement between the actuator coils and the permanent magnet. The actuator has a coil body divided into two equal halves, with the left half of the coil containing a left-handed wound of enamelled copper conductor and the right half of the coil containing a clockwise-wound winding of the same enamelled copper conductor. Both coils are electrically connected in series, which creates a magnetic field with three poles when the same electric current passes through these coils, with two poles at each end of the coil and one in the middle of the coil between the windings. After inserting the core from the rod axially polarized permanent

magnet into this coil, the magnetic field of the coil and the permanent magnet interact, and thus, its movement depends on the polarization of the coil and the permanent magnet. The length of the coil with both windings is twice the length of the permanent magnet, and so when moving, the magnet is moved between two extreme positions inside the device. Attached to the permanent magnet are threaded rods with suspension eyes, by means of which it is possible to transmit the movement of the permanent magnet to the device to be moved (Figure 1) [6].



1 - Permanent magnet in the housing; 2 - Threaded adapter; 3 - Threaded rod; 4 - Actuator stroke adjustment nut; 5 - Actuator hanging eye; 6 - Actuator coil body; 7 - Left winding of the actuator coil; 8 - Right winding of the actuator coil; 9 - Actuator cover

Figure 1 Linear electromagnetic solenoid actuator arrangement

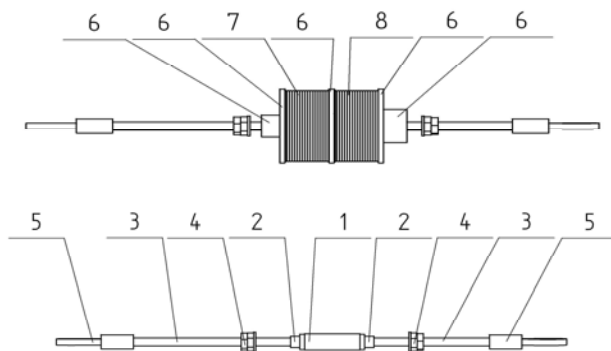
**LINEAR SOLENOID ELECTROMAGNETIC ACTUATOR WITH DIFFERENTIAL SERIES WINDINGS**

Tatiana Kelemenová; Ivana Koláriková; Ondrej Benedik

The advantage of the solution is that, unlike conventional solenoid actuators, which consist of a ferromagnetic core with a single-coil, this actuator contains a rod axially polarized permanent magnet with two differential series-connected windings, which allows greater force effects while making better use of the permanent magnet magnetic field.

### 3 Actuator implementation

A prototype of a linear solenoid electromagnetic actuator with differential series-connected windings and a permanent magnet (figs. 2, 3) was created, which consists of a permanent magnet (1) in housing and which is connected on both sides by riveting to threaded spacers (2). A threaded rod (3) with the actuating eyes (5) of the actuator is attached to both threaded spacers (2). Nuts (4) for adjusting the actuator stroke are also located on the threaded rods (3). The assembly of the permanent magnet (1) in the housing, threaded spacers (2), threaded rod (3), nuts (4) for adjusting the actuator stroke and actuator eyelets (5) forms a moving part of the actuator and is inserted into the carcass hole (6) actuator coils. The actuator coil body (6) comprises a left actuator coil winding (7) and a right actuator coil winding (8), the sense of winding the left actuator coil winding (7) being opposite to the right actuator coil winding (8), thus achieving a specific magnetic arrangement coil field. The frame (6) of the actuator coil, the left winding (7) of the actuator coil and the right winding (8) of the actuator coil are covered by the actuator cover (9) (Figure 2).



1 - Permanent magnet in the housing; 2 - Threaded adapter; 3 - Threaded rod; 4 - Actuator stroke adjustment nut; 5 - Actuator hanging eye; 6 - Actuator coil body; 7 - Left winding of the actuator coil; 8 - Right winding of the actuator coil; 9 - Actuator cover

Figure 2 Actuator winding and plunger with permanent magnet

After activating the actuator by the passing current, a magnetic field is created around the left winding (7) of the actuator coil, and the right winding (8) of the actuator coil and the interaction of the magnetic field of the permanent magnet (1) in the housing creates actuator stroke. The actuator stroke can be adjusted using the actuator stroke adjustment nuts (4) according to the needs and application of the device. The frame (6) of the actuator coil comprises

on both sides a mounting shoulder for application. It is assumed that the frame (6) of the actuator coil is firmly held as a non-moving part. The moving part of the actuator consisting of a permanent magnet (1) in the housing, threaded spacers (2), threaded rod (3) and nuts (4) for adjusting the actuator stroke and actuator eyelets (5) is attached by means of actuator eyelets (5), to the moving part of the selected application (Figure 2, Figure 3).

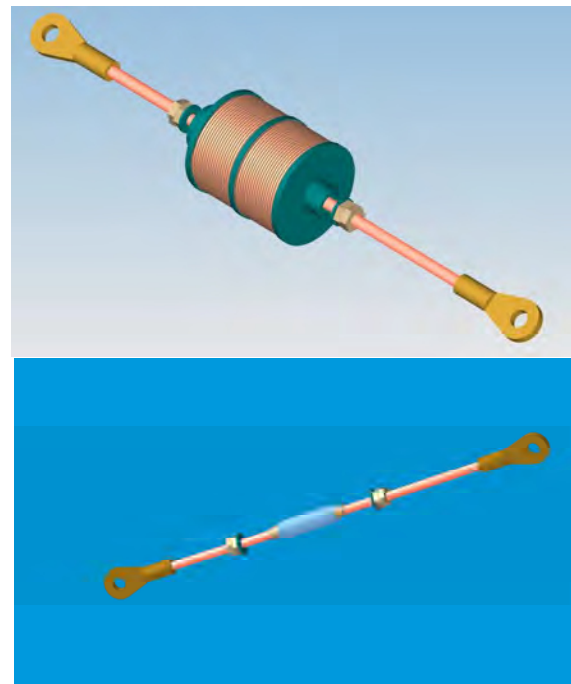


Figure 3 Virtual model of the actuator and permanent magnet

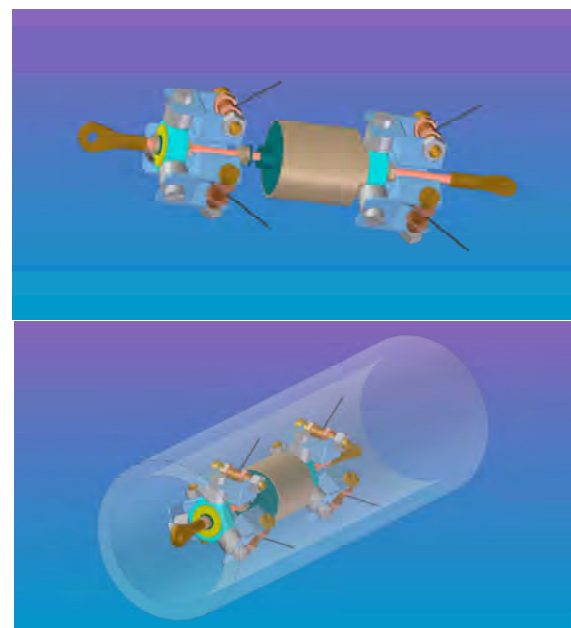


Figure 4 Implementation of an in-pipe robot for locomotion in the pipeline

**LINEAR SOLENOID ELECTROMAGNETIC ACTUATOR WITH DIFFERENTIAL SERIES WINDINGS**

Tatiana Kelemenová; Ivana Koláriková; Ondrej Benedik

The device, according to the proposed solution, can be used to create a linear reciprocating motion with a force effect in applications where it is necessary to move the masses between two defined end positions. An example of such an application is an in-pipe robot for moving in a pipeline, which uses this actuator to perform a movement in the pipeline in order to transport objects to the pipeline or inspect the pipeline (Figure 4).

**4 Experimental examination**

The aim was to experimentally investigate the traction force of such an actuator depending on the position of the magnet relative to the actuator coil. The design of the actuator (Figure 5) is designed for application in an in-pipe robot. The permanent magnet is axially polarized and is made of NdFeB material. During the measurement, the actuator was held in a holder, and the ends of the permanent magnet were attached to a bowl with weights using a system of cable and pulley. Using a suitable combination of weights, a loading force was created, and the actuator was tested in the experiment to see if it could exert a force to lift this weight (Figure 6).

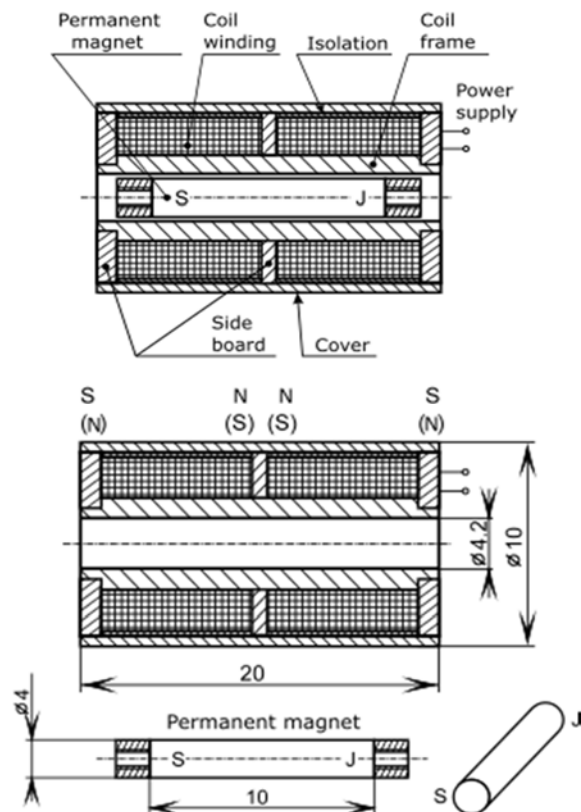


Figure 5 Arrangement and dimensions of the actuator coil and magnet

The actuator was excited by a constant electric current, which was shaped by the control unit in the form of switching pulses. Excitation by a constant electric current is very important because due to the flowing current, the

coil of the actuator winding heats up and thus its electrical resistance changes, which would mean a decrease in the magnitude of the electric current when excited by a constant voltage source since it is known from electromagnetic field theory that the strength of the magnetic field depends on the electric current flowing through the coil of the actuator winding.

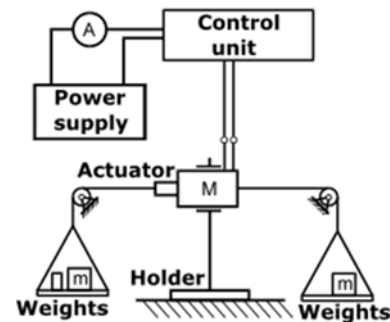


Figure 6 Measuring chain arrangement

The actuator loading was performed first from the left side and then from the right side (Figure 6). The load was increased by adding weight until the maximum weight that the actuator was able to lift at the set position of the permanent magnet relative to the actuator coil was determined. The maximum developed force of the actuator was 0.85 N when excited by a constant electric current of 1A and corresponded to the central position of the permanent magnet with respect to the centre of the actuator coil. The measured values were approximated only by the spline curve, as it is quite complicated to describe this course by one regression function (Figure 7).

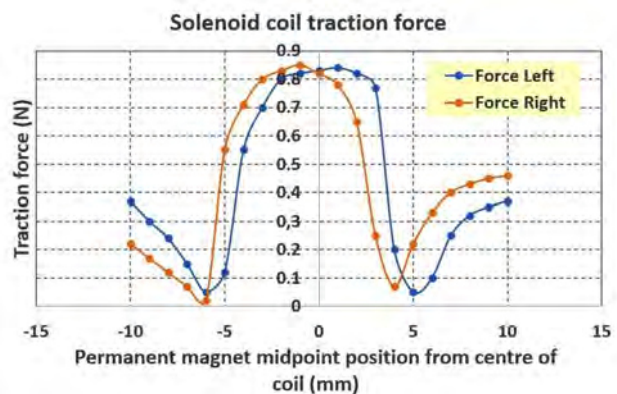


Figure 8 Dependence of the traction force of the actuator on the position of the centre of the permanent magnet relative to the centre of the coil

From previous measurements (Figure 8), it is clear that the optimal position for the use of the actuator in terms of achieving the maximum value of traction force is when the centre of the permanent magnet is in the centre of the actuator coil.

**LINEAR SOLENOID ELECTROMAGNETIC ACTUATOR WITH DIFFERENTIAL SERIES WINDINGS**

Tatiana Kelemenová; Ivana Koláriková; Ondrej Benedik

When applying this actuator, it will perform a certain stroke around this optimal position. This mechanical work will therefore be used for a specific application. From the point of view of the application, it is important to know the dependence of the magnitude of the traction force on this stroke. It is assumed that the achievable force will decrease with larger strokes.

This experiment was carried out in such a way that the stroke limit was set with the adjusting screws, and the actuator was tested for the maximum load that the actuator was still able to develop.

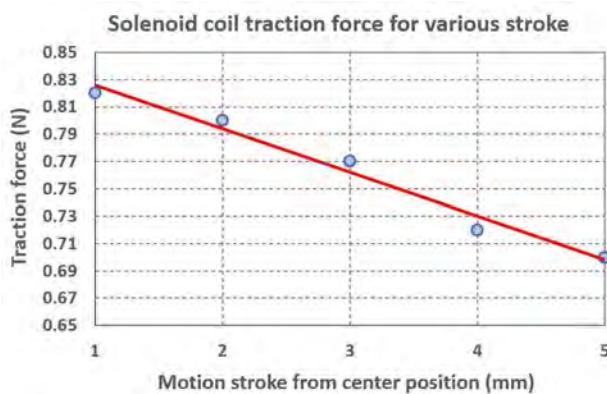


Figure 9 Dependence of the traction force of the actuator at the stroke height around the centre position of the coil

The experiments (Figure 9) confirmed that the traction force decreases with increasing stroke as the permanent magnet moves further away from the centre of the coil. This dependence therefore makes it possible to assess the suitability of this actuator for a particular application. If the required stroke is known, then it is possible to determine the traction force that can be developed by this actuator.

## 5 Conclusion

The obtained experimental dependence shows:

1. The functional dependence acquires in the middle position (the radial axis of the magnetic core is identical with the radial axis of the coil). This is shown as a significant extreme, i. weight of weight resp. the equivalent force with which the actuator can still move.

2. The whole magnetic core is inserted into the coil in the working position, which makes much more use of the magnetic properties of the permanent magnet.

The designed arrangement of the solenoid actuator thus provides energetically better use of the magnetic field of the permanent magnet coil. This fact can be an advantage, especially with miniaturized sizes of this type of actuator [7-24].

## Acknowledgement

The work has been accomplished under the research project VEGA 1/0168/21 and KEGA 016TUKE-4/2021 financed by the Slovak Ministry of Education.

## References

- [1] Yao, F., H., FAN, R.L., QI, S.Q.: *Theoretical Study and Experimental Test on Solenoid Actuator of Active Control Mount*, Advances in Intelligent Systems and Computing Volume 1305 AISC, Pages 119 - 130 2021 2<sup>nd</sup> International Symposium on Simulation and Process Modelling, ISSPM 2020 Shenyang 29 August 2020 through 30 August 2020 Code 257579, 2020. [https://doi.org/10.1007/978-981-33-4575-1\\_12](https://doi.org/10.1007/978-981-33-4575-1_12)
- [2] WU, L., LU, K.: A development study of a new bi-directional solenoid actuator for active locomotion capsule robots, *Electronics*, Vol. 9, No. 5, pp. 1-14, 2020. <https://doi.org/10.3390/electronics9050736>
- [3] EBRAHIMI, N., SCHIMPF, P., JAFARI, A.: Design optimization of a solenoid-based electromagnetic soft actuator with permanent magnet core, *Sensors and Actuators, A: Physical*, Vol. 284, pp 276-285, 2018. <https://doi.org/10.1016/j.sna.2018.10.026>.
- [4] PLAVEC, E., PETRENIC, M., VIDOVIC, M.: Improving the Force and Time Response of a DC Solenoid Electromagnetic Actuator by Changing the Lower Core Angle, *Journal of Electromagnetic Engineering and Science*, Vol. 21, No. 2, pp. 95-103, 2021. <https://doi.org/10.26866/jees.2021.21.2.95>.
- [5] UGAROV, G.G., VYRYKHANOV, D.A., MOSHKIN, V.I., MOROZOV, P.V.: Numerical simulation of the efficiency of magnetic energy conversion in linear electromagnetic converters, *Journal of Physics: Conference Series*, Vol. 2032, No. 118, 2021, Article number 012089 2021 International Conference on IT in Business and Industry, ITBI 2021 Novosibirsk 12 May 2021 through 14 May 2021 Code 173043. <https://doi.org/10.1088/1742-6596/2032/1/012089>
- [6] VIRGALA, I., et all: Linear solenoid electromagnetic actuator with differential series-connected windings and permanent magnet, *Patent application*, No.: SK 288550 B6. Application date: Jan. 28<sup>th</sup>, 2016.
- [7] KELEMENOVÁ, T., FRANKOVSKÝ, P., VIRGALA, I., MIKOVÁ, Ľ., KELEMEN, M.: Machines for Inspection of Pipes, *Acta Mechatronica*, Vol. 1, No. 1, pp. 1-7, 2016.
- [8] KELEMEN, M., MIKOVÁ, Ľ., HRONCOVÁ, D., FILAKOVSKÝ, F., SINČÁK, P.J.: Embedded Systems – Control of Power Subsystems, *Acta Mechatronica*, Vol. 5, No. 2, pp. 23-28, 2020.
- [9] PAPACZ, W.: Didactic Models of Manipulators, *Acta Mechatronica*, Vol. 3, No. 3, pp. 7-11, 2018.
- [10] KURYŁO, P.: Experimental Stand for Actuator Testing, *Acta Mechatronica*, Vol. 3, No. 2, pp. 7-10, 2018.
- [11] BOŽEK, P.: Robot path optimization for spot welding applications in automotive industry, *Tehnicki vjesnik / Technical Gazette*, Vol. 20, No. 5, pp. 913-917, 2013.
- [12] DUCHOŇ, F., BABINEC, A., KAJAN, M., BEŇO, P., FLOREK, M., FICO, T., JURIŠICA, L.: Path

**LINEAR SOLENOID ELECTROMAGNETIC ACTUATOR WITH DIFFERENTIAL SERIES WINDINGS**

Tatiana Kelemenová; Ivana Koláriková; Ondrej Benedik

- planning with modified a star algorithm for a mobile robot, *Procedia Engineering*, Vol. 96, pp. 59-69, 2014.
- [13] PÁSZTÓ, P., HUBINSKÝ, P.: Mobile robot navigation based on circle recognition, *Journal of Electrical Engineering*, Vol. 64, No. 2, pp. 84-91, 2013.
- [14] ABRAMOV, I.V., NIKITIN, Y.R., ABRAMOV, A. I., SOSNOVICH, E.V., BOŽEK, P.: Control and Diagnostic Model of Brushless DC Motor, *Journal of Electrical Engineering*, Vol. 65, No. 5, pp. 277-282, 2014.
- [15] KONIAR, D., HARGAŠ, L., ŠTOFAN, S.: Segmentation of Motion Regions for Biomechanical Systems, *Procedia Engineering*, Vol. 48, pp. 304-311, 2012.
- [16] KARAVAEV, Y.L., KILIN, A.A.: Nonholonomic dynamics and control of a spherical robot with an internal omniwheel platform: Theory and experiments, *Proceedings of the Steklov Institute of Mathematics*, Vol. 295, No. 1, pp. 158-167, 2016.
- [17] VIRGALA, I., MIKOVÁ, Ľ., KELEMEN, M., HRONCOVÁ, D.: Snake-like robots, *Acta Mechatronica*, Vol. 3, No. 4, pp. 7-10, 2018.
- [21] MIKOVÁ, Ľ., VIRGALA, I., KELEMEN, M.: Embedded systems, *Acta Mechatronica*, Vol. 3, No. 2, pp. 1-5, 2018.
- [22] KELEMENOVÁ, T., FRANKOVSKÝ, P., VIRGALA, I., MIKOVÁ, Ľ., KELEMEN, M., DOMINIK, L.: Educational models for mechatronic courses, *Acta Mechatronica*, Vol. 1, No. 4, pp. 1-6, 2016.
- [23] LIPTÁK, T., KELEMEN, M., GMITERKO, A., VIRGALA, I., HRONCOVÁ, D.: The control of holonomic system, *Acta Mechatronica*, Vol. 1, No. 2, 2016, pp. 15-20.
- [24] KURYĽO, P., PIVARČIOVÁ, E., CYGANIUK, J., FRANKOVSKÝ, P.: Machine vision system measuring the trajectory of upper limb motion applying the Matlab software, *Measurement Science Review*, Journal of Institute of Measurement Science of Slovak Academy of Sciences, Vol. 19, No. 1, pp. 1-8, 2019.

**Review process**

Single-blind peer review process

# SOFTWARE APPLICATION FOR A SYSTEM WITH A PROGRAMMABLE LOGIC CONTROLLER

**Jaroslav Romančík**

Technical University of Kosice, Faculty of Mechanical Engineering, Letna 9, Kosice, Slovak Republic, EU,  
jaroslav.romancik.2@tuke.sk (corresponding author)

**Michal Kelemen**

Technical University of Kosice, Faculty of Mechanical Engineering, Letna 9, Kosice, Slovak Republic, EU,  
michal.kelemen@tuke.sk

**Keywords:** PLC, HMI, control system, ladder

**Abstract:** The article deals with the solution of an application for a building security system, which is solved using a programmable logic controller. A ladder program design for this application is created, and an application for the HMI touch screen is also designed. The application is tested on a simulation model in a software development environment. A training station system was used for practical prototype tests, which includes a programmable logic controller, HMI touch screen, profinet switch, power supply and other accessories for testing purposes.

## 1 Introduction

The gradual development of human society has also been reflected in the expansive development of modern technologies, which have become an integral part of our lives. We got used to most of the gains so quickly that we took them for granted. This fact does not only affect ordinary computers, mobile phones or other white goods. It works similarly in industrial engineering.

Without the use of automation elements, production, as we know it today, would not be possible. It would not be possible to produce so many products in such a short time, with such precision, if all these tasks were to be done by man. We have to admit that machines are more efficient. But still, there has to be a person at the top. In this particular case, the PLC programmer. As PLC (acronym from Programmable Logic Controller) is a frequently used tool for controlling robotic arms, conveyor belts and entire lines, it has also become a major player in mechatronics.

The implementation of PLCs began in the 80s of the 20th century, but their origin dates back to the 70s. The first company to address this issue was General Motors. In 1968, it announced a competition, the task of which was to build a control system as a replacement for the hitherto used relay, the reprogramming ability of which depended on the design and electronic connection. If changes were to be made in the activities, the cabling had to be changed, which was still often very confusing. Also, the switching of the relay is not infinite and has a limited number of cycles. Therefore, finding the relay that was not working caused a lot of maintenance problems.

Today, human activities are often replaced by machines. Since the trend is to mechanize and automate, a great means has proven to be PLC automation. We can meet him in every part of the industry, from the control of conveyor belts and robotic arms in the automotive industry, through the automation of filling and transfer machines in the food industry, to applications in smart homes from

water heating to the opening of windows depending on the time of day. They are mainly used in places of industry where it is necessary to work with a large amount of information from sensors, as they offer a large number of inputs and outputs, whether digital or analog (Figure 1). Also, the PLC version is very advantageous, as they can be easily enclosed in a large box, called a rack, and so they can be placed in larger halls. In this way, they are protected from unauthorized access. Also, the entire main cabling can be stored in this way, which protects the entire system from moisture, dust, other electronic devices or vibrations.



Figure 1 PLC in conjunction with sensors, actuators, controls and output modules

HMI touch screens (Human-machine interface - HMI panel), which are currently an integral part of the PLC, are also used together with the PLC. HMI touch screens are devices with sensitive touch screens for operator input and are usually mounted so that they can be operated by personnel or operator. They provide a visual graphical interface with up-to-date information about the controlled device and controls and allow easy operation and selection of device operation options [1-3].

## 2 Building security system

A security system is proposed for the complex, which will be monitored by staff (Figure 2). The complex has three possible inputs. During the day, people and employees enter the complex, but after a certain hour, when the staff activates the security system, no one will be allowed to enter the building without triggering an alarm. If someone still enters the building, an audible alarm will sound, accompanied by warning lights. The staff will also need to know the exact location of the breach in order to intervene properly. The created program will have to be executable and stoppable in the HMI display environment, as it should only work at a certain time of day. We also have to count on three entrances to the complex, the opening or closing of which we will simulate with the buttons. If the intruder enters the complex, this security breach will trigger the siren, which will simulate an audible alarm, and light up the LEDs on the training module, which will simulate the warning lights. The entire condition of the building will be monitorable using the HMI panel.



Figure 2 Building security system

In order to be able to work with PLC and HMI panel and to be able to create programs, it is necessary to set the device configuration in the environment where we create a program with these two devices and possibly add later modules if necessary to expand the device. The individual modules can be connected via the Profinet interface (Figure 3).

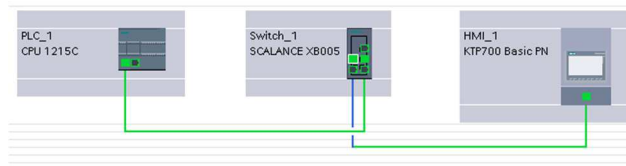


Figure 3 Topology of PLC and HMI devices

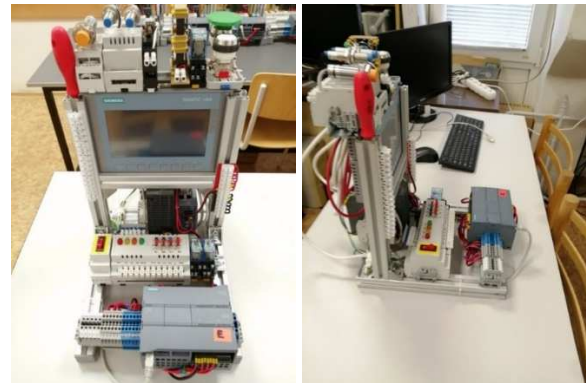


Figure 4 Training station with PLC and HMI panel

For prototype tests, it is then possible to use a training station with a PLC (Figure 4), which contains a PLC core module, HMI touch screen, industrial switch, power supply and other testing accessories such as switches, LED indicators, sensors, motors, solenoids, etc. [4-6].

## 3 Program design

The program is often implemented using the Ladder logic language, which is considered to be the simplest form of PLC programming. Ladder logic has evolved into a programming language that represents a program using a graphical scheme based on relay logic hardware circuit diagrams. Ladder logic is used to develop software for programmable logic controllers (PLCs) used in industrial control applications. The name is based on the observation that programs in this language resemble ladders with two vertical rails and a series of horizontal bars between them. Whereas Ladder logic was once the only available entry for recording programmable controller programs, today, other forms are standardized in the IEC 61131-3 standard.

The solved alarm system should be switchable and switchable via the HMI panel. This function will be implemented using a switch. In order to make it clear what state the security system is in, this state will be indicated by the LEDs of the training module, as well as by the information on the HMI display. We will start with a Normally open contact, which we will call "start", which will be the input. We will store an assignment for it, which we will call "m\_start" and it will be a memory variable that will be used for the HMI panel. We end this part with the output "alarm\_functional", which in our case lights up the green LED diode. This part of the program will be used to turn on the security system. We will use a similar procedure to turn it off, but in this case we will use the Normally closed contact, but we will use the same input. By turning it off, we will switch the assignment "alarm\_nofunctional", which will cause the red LED to light up (Figure 5).

**SOFTWARE APPLICATION FOR A SYSTEM WITH A PROGRAMMABLE LOGIC CONTROLLER**

Jaroslav Romančík; Michal Kelemen

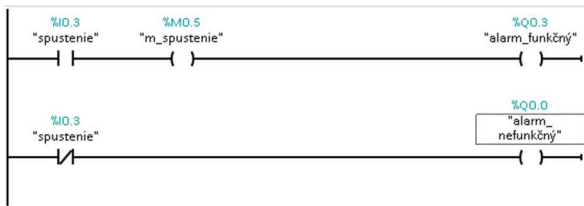


Figure 5 Ladder program - start and stop

In the next step, we will create the main part of the program. Because there are three entrances to the complex. We will monitor their opening and closing in our program using Normally open contact. We will create a separate branch in the program for each entrance. For easier orientation, we will call them, for example, "main\_entrance", "secondary\_entry", "garage\_doors". Since we will also want to see their status on the HMI display, we will place an assignment as a memory variable for each input. In order to distinguish the individual memory variables and their assignment to the individual inputs, we will call them "m\_main\_input", "m\_side\_input" and "m\_garage\_doors". In order for our program to work properly and fully, it is necessary to realize that after the first alarm, the alarm must remain on, even if the entrance closes. We solve this problem using the logical operator Counter, specifically CTU (Count up), ie count up. After placing this block in Ladder, we can notice that this operator has its own inputs and outputs. CU serves as input, Q as output. PV determines the value by which the counter should count, the CV from which value it starts. R indicates reset. We substitute a value of 0 for CV, and a value of 1 for PV, which we achieve when the signal is applied by pressing the button to count the counter to 1, and even after releasing the button to keep the logic 1 at the output. If we want to reset it, we connect the "start" input to the R terminal. This will ensure that after the alarm is triggered, we reset it by turning off the security system, otherwise the alarm will remain triggered. We will use counters for each entrance. After Q we will add another memory variable, which will be needed when programming the HMI panel. We will end this whole part of the program with the "alarm" output, for which we will use the assignment operator, and it will be common for all three entrances. We will switch the siren on this operator. After that, we place the memory variable "m\_alarm", which will display the alarm on the HMI display (Figure 6).

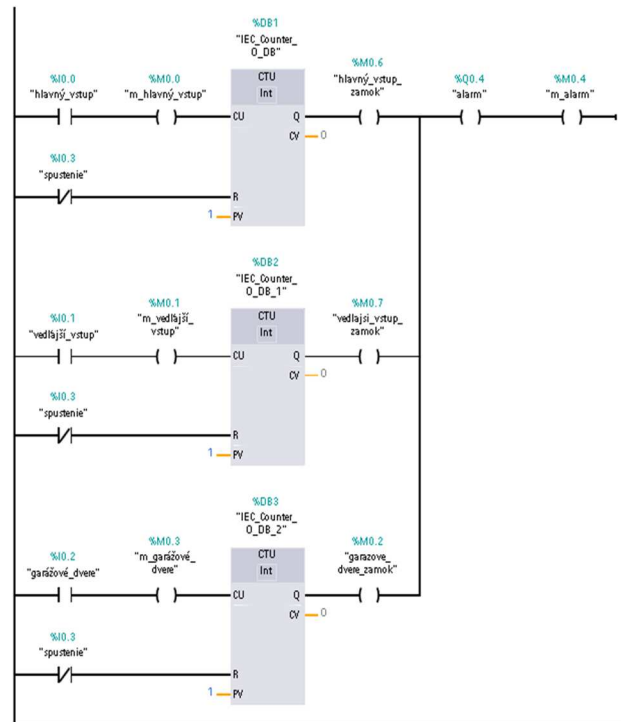


Figure 6 Ladder program - the main part of the program

The last part of the Ladder program will be the creation of signalling by means of LED diodes, announcing that the alarm has been triggered. For better signalling of the alarm, we will design the program so that the two remaining LEDs (orange and yellow) flash. You will need to use timers to blink. We start the program with the "alarm" output, which ended the previous part of the program, but this time we will use the contact normally open. From this step, it is clear that the flashing will be triggered, and only if the alarm is triggered. We will create two branches for individual LEDs. We start each branch with a TON timer. If we look at the timer, we find the designation IN, which means input. Q indicates output. PT and ET set the start and end time by how long the input signal is to be delayed. In this case, we will use a time of 2 to 0 seconds. In the first branch we add a timer identical to the previous one, but not in the second branch. This step will cause one LED to be shifted by 2 seconds, compared to the other. If we did not add this timer to our program, both LEDs would flash at the same time. Next we will add outputs for individual LED diodes. We will call them "warning\_light\_1" and "warning\_light\_2". They will be followed by other timers, with identical parameters as the previous ones. We end the program with RT (reset timer) operators, two for each branch. These operators have the task of resetting the timers, so that the LEDs in the loop flash. We will only reset the timers before and after the diodes, so we will not reset the first timer in the branch with three timers, as its task was only to shift the flashing frequency of one of the LEDs once (Figure 7).

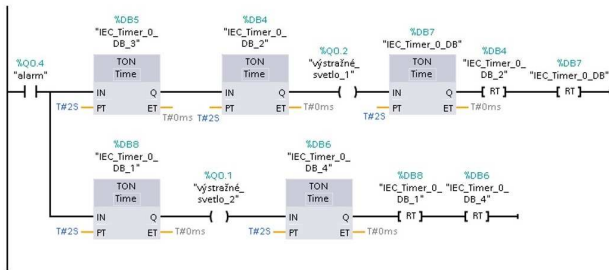


Figure 7 Ladder program - flashing LEDs

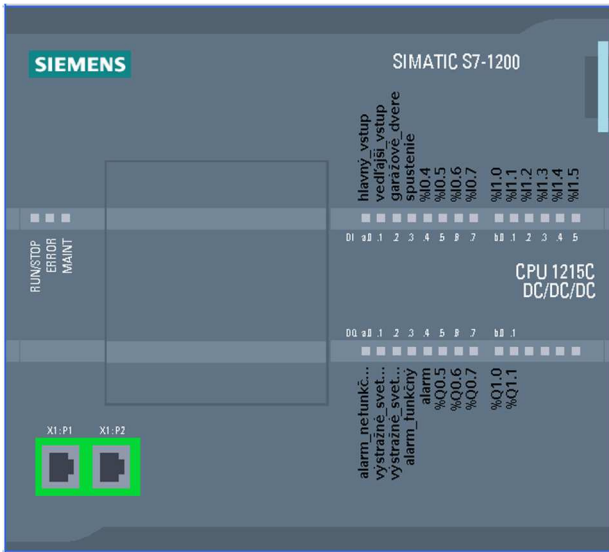


Figure 8 Virtual digital twin after program creation

After creating the entire Ladder program, we can notice that all the inputs and outputs we use are displayed on the virtual digital twin of our PLC (Figure 8). This display can help us to connect inputs and outputs using wires between the PLC and the training module. The next step will be loading the program into the PLC.

#### 4 Program design for HMI panel

In the next step we will create a program for the HMI panel. For this particular solution, the appearance of the HMI with a dark blue background was chosen, with a home and sub screen and two buttons, one to turn off the program and the other to return to the home screen of the HMI panel (Figure 9).

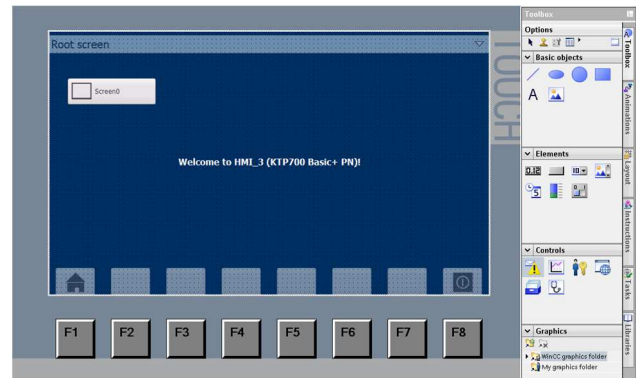


Figure 9 HMI design

We will create a graphical design of the HMI interface by placing graphical objects and their subsequent connection with events and visualization conditions via HMI tags connected to PLC tags. The visibility of individual objects can be solved using the functions Dynamize colors and flashing and Make visibility dynamic (Figure 10).

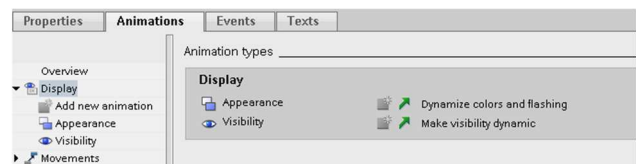


Figure 10 Visualization of objects

The first function of the program should be the ability to turn the security system on or off. Therefore, in our case, the inscription "INACTIVE" was created. It is made up of two parts. The word NO is visible in the logical state zero of the "HMI\_start" tag, but one is invisible in the logical state. The same tag is also used for the second part of the word "ACTIVE". But in this case, it is red at logical zero, and green at logical unit. In this way, personnel can see the status of the security system not only by means of LED diodes, but also by a colored sign. Since he has to see where the violation occurred, we will create a table called "PLACE OF INFRINGEMENT". It contains three columns, namely "MAIN ENTRANCE", "SIDE ENTRANCE" and "GARAGE DOOR", with lock icons in front of each sign. They will be controlled by the tags: "HMI\_main\_entry\_input", "HMI\_current\_entry\_input", "HMI\_garazove\_door\_lock". If the logical state is zero on them, they will be invisible. However, if the object is disturbed, the panel will display the label, depending on where the alarm was triggered. "ALARM" is invisible unless an alarm is triggered. If it has occurred, the inscription will appear and flash alternately red and yellow. The beacon above the word "ALARM" is made up of three identical images that overlap, are layered, and are white, red, and yellow. If the alarm is not triggered, a white beacon is visible, red and yellow are invisible. However, when the alarm is triggered, the white beacon disappears, becomes invisible, but the red and yellow beacons are

**SOFTWARE APPLICATION FOR A SYSTEM WITH A PROGRAMMABLE LOGIC CONTROLLER**

Jaroslav Romančík; Michal Kelemen

visible. The yellow beacon, placed in the top layers, also flashes. This creates the illusion that when the alarm is triggered, the off white beacon will flash alternately red and yellow. In this way, the staff will be clearly informed that the complex has been disrupted. The beacon and the inscription "ALARM" are controlled by the logical state of the tag: "HMI\_alarm". We will rename the "Screen" button, which will take us to the new screen, by a more appropriate name. In our case, the inscription: "GUARDED OBJECT" (Figure 11).

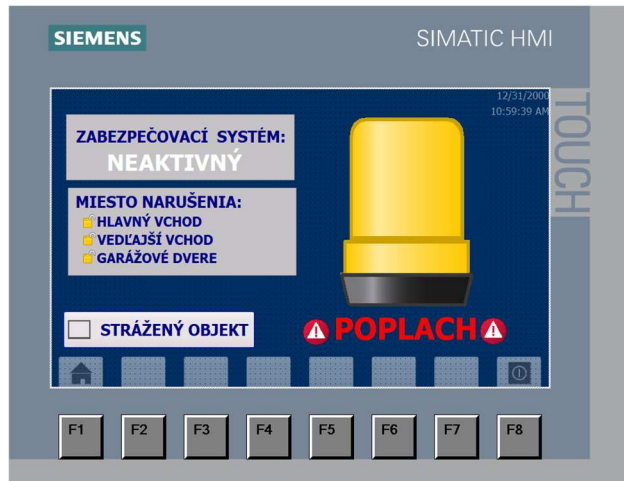


Figure 11 Graphic design HMI- Root screen

In the next step, we will create a graphical display of the screen, which we will be able to access using the "GUARDED OBJECT" button. On this screen, staff will be able to see the entire complex with the exact location of the individual entrances to the complex. He will also see the door open and close during the day, whether or not the security system is active.

Using images of buildings and the outside environment, we will create the appearance of a complex that will always be visible. We will add pictures of the door. We choose two for each entrance, when the door is open and when it is closed. We program the image of closed doors so that at logic state zero, the image is visible, but at logic state one is invisible. We program the image of the open entrance in reverse. After stacking them on top of each other and placing them in the appropriate place of the complex, the illusion of opening and closing the door arises. We will use this procedure for all entrances. They will be controlled by the tags: "HMI\_main\_input", "HMI\_side\_input" and "HMI\_garage\_doors".

As personnel see the current state of the door, they must know where the alarm was triggered, even though the intruder managed to close the door. Therefore, we will add a table with the names of the entrances along with the lock icons and a warning triangle with an exclamation mark above each door. If the security system is active and the complex is disturbed, a warning symbol will appear above the specific entrance and will flash, regardless of whether

the door is closed or open. The lock icon will only be visible if the door has been opened. Their function will be controlled by the same tags that we used to program the table "DISTRIBUTION LOCATION", namely: "HMI\_main\_input\_input", "HMI\_additional\_lock\_input", "HMI\_garazove\_door\_locks". At the bottom of the screen is the "HOME" button. This button takes you back to the home page (Figure 12).

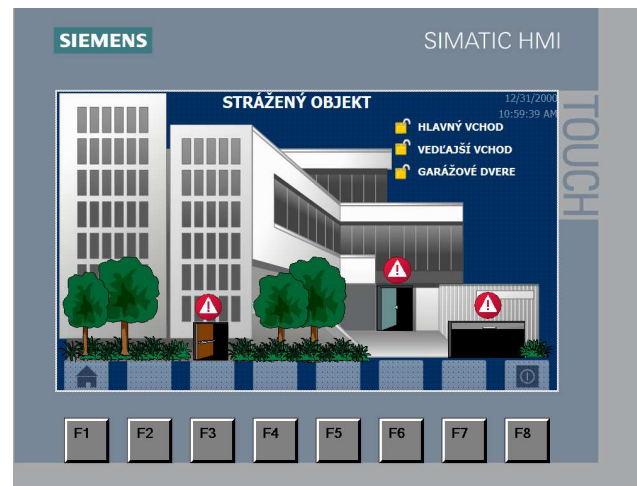


Figure 12 Graphic design HMI- Guarded object

As in the case of loading a program for a PLC, the program for the HMI panel must first be compiled, and then we will perform a loading into the HMI panel device. After loading we can test its functionality. After a successful simulation in the program environment, the implementation into the training station and the successful testing of the proposed program were also successful.

## 5 Conclusion

PLC systems are located in switchboards together with other electrical modules and are not normally accessible to ordinary users. For communication with the user, the PLCs are equipped with a Human-machine interface (HMI), which allows the user to control the status of the controlled system and can intervene in the control process if the situation in the controlled process so requires.

PLC control systems are installed in devices with high electrical voltage, where there is a risk of electric shock and thus only the technician who has the appropriate authorizations in connection with the safety of work with electrical equipment has direct access to the hardware of PLC control systems. In many cases, the controlled system is a technological system, the costs of which are high, so it is important that only authorized persons work with the PLC control system [7-17].

## Acknowledgement

The work has been accomplished under the research project KEGA 030TUKE-4/2020 financed by the Slovak Ministry of Education.

## SOFTWARE APPLICATION FOR A SYSTEM WITH A PROGRAMMABLE LOGIC CONTROLLER

Jaroslav Romančík; Michal Kelemen

**References**

- [1] LANDER, A.: *Programmable Logic Controllers: The Evolution of a Disruptive Technology*, Engineering.com, [Online], Available: <https://new.engineering.com/story/programmable-logic-controllers-the-evolution-of-a-disruptive-technology> [26 May 2021], 2021.
- [2] SIMATIC S7-1200 *Getting started with S7-1200*, [Online], Available: [https://cache.industry.siemens.com/dl/files/875/39644875/att\\_76194/v1/s71200\\_getting\\_started\\_en-US\\_en-US.pdf?download=false](https://cache.industry.siemens.com/dl/files/875/39644875/att_76194/v1/s71200_getting_started_en-US_en-US.pdf?download=false) [26 May 2021].
- [3] SIMATIC S7-1200 *Programming Guideline for S7-1200/1500*, [Online], Available: <https://assets.new.siemens.com/siemens/assets/api/uuid:c7de7888-d24c-4e74-ad41-759e47e4e444/Programovani-S7-1200-1500-2018.pdf> [26 May 2021], 2021.
- [4] KELEMEN, M., SINČÁK, P.J.: Programmable logic controller training stands for educational purposes, *Technical Sciences and Technologies*, Vol. 21, No. 3, pp. 274-280, 2020.
- [5] KELEMEN, M., LIGUŠOVÁ, J., LIGUŠ, J., MAXIM, V.: Additional Modules for Programmable Logic Controller Based Training Stands, *Technical Sciences and Technologies*, Vol. 22, No. 4, pp. 170-176, 2020.
- [6] KELEMEN, M., KELEMENOVÁ, T., VIRGALA, I., PRADA, E., MIKOVÁ, E., HRONCOVÁ, D., VARGA, M., SINČÁK, P.J.: *Training stations with programmable logic controllers*, Technological Forum 2021: 12<sup>th</sup> International technical conference: 30.6. - 02.07.2021, Jaroměř, ČR, pp. 117-121, 2021.
- [7] VITKO, A., JURÍŠICA, L., KLÚČÍK, M., MURÁR, R., DUCHOŇ, F.: Embedding Intelligence into a Mobile Robot, *AT&P Journal Plus*, Vol. 2008, No. 1, Mobile robotic systems, pp. 42-44, 2008.
- [8] BOŽEK, P.: Robot path optimization for spot welding applications in automotive industry, *Tehnicki vjesnik / Technical Gazette*, Vol. 20, No. 5, pp. 913-917, 2013.
- [9] DUCHOŇ, F., BABINEC, A., KAJAN, M., BEŇO, P., FLOREK, M., FICO, T., JURÍŠICA, L.: Path planning with modified a star algorithm for a mobile robot, *Procedia Engineering*, Vol. 96, pp. 59-69, 2014.
- [10] PÁSZTÓ, P., HUBINSKÝ, P.: Mobile robot navigation based on circle recognition, *Journal of Electrical Engineering*, Vol. 64, No. 2, pp. 84-91, 2013.
- [11] ABRAMOV, I.V., NIKITIN, Y.R., ABRAMOV, A.I., SOSNOVICH, E.V., BOŽEK, P.: Control and Diagnostic Model of Brushless DC Motor, *Journal of Electrical Engineering*, Vol. 65, No. 5, pp. 277-282, 2014.
- [12] KONIAR, D., HARGAŠ, L., ŠTOFAN, S.: Segmentation of Motion Regions for Biomechanical Systems, *Procedia Engineering*, Vol. 48, pp. 304-311, 2012.
- [13] VIRGALA, I., MIKOVÁ, E., KELEMEN, M., HRONCOVÁ, D.: Snake-like robots, *Acta Mechatronica*, Vol. 3, No. 4, pp. 7-10, 2018.
- [14] MIKOVÁ, E., VIRGALA, I., KELEMEN, M.: Embedded systems, *Acta Mechatronica*, Vol. 3, No. 2, pp. 1-5, 2018.
- [15] KELEMENOVÁ, T., FRANKOVSKÝ, P., VIRGALA, I., MIKOVÁ, E., KELEMEN, M., DOMINIK, L.: Educational models for mechatronic courses, *Acta Mechatronica*, Vol. 1, No. 4, pp. 1-6, 2016.
- [16] LIPTÁK, T., KELEMEN, M., GMITERKO, A., VIRGALA, I., HRONCOVÁ, D.: the control of holonomic system, *Acta Mechatronica*, Vol. 1, No. 2, pp. 15-20, 2016.
- [17] KURYŁO, P., PIVARČIOVÁ, E., CYGANIUK, J., FRANKOVSKÝ, P.: Machine vision system measuring the trajectory of upper limb motion applying the Matlab software, *Measurement Science Review*, Journal of Institute of Measurement Science of Slovak Academy of Sciences, Vol. 19, No. 1, pp. 1-8, 2019.

**Review process**

Single-blind peer review process



## JOURNAL STATEMENT

---

Journal name:	<b>Acta Mechatronica</b>
Abbreviated key title:	Acta Mechatron
Journal title initials:	AM
Journal doi:	10.22306/am
ISSN:	2453-7306
Start year:	2016
The first publishing:	March 2016
Issue publishing:	Quarterly
Publishing form:	On-line electronic publishing
Availability of articles:	Open Access Journal
Journal license:	CC BY-NC
Publication ethics:	COPE, ELSEVIER Publishing Ethics
Plagiarism check:	Worldwide originality control system
Peer review process:	Single-blind review at least two reviewers
Language:	English
Journal e-mail:	<b>info@actamechatronica.eu</b>

The journal focuses mainly on original, interesting, new and quality, theoretical, practical and application-oriented contributions to the scientific fields and research as well as to pedagogy and training in mechatronics.

Publisher:	<b>4S go, s.r.o.</b>
Address:	Semsa 24, 044 21 Semsa, Slovak Republic, EU
Phone:	+421 948 366 110
Publisher e-mail:	<b>info@4sgo.eu</b>

**Responsibility for the content of a manuscript rests upon the authors and not upon the editors or the publisher.**